Phase Diagram and Electrical Conductivity of the AgCl-NdCl$_3$ Binary System

Monika Szymanska-Kolodziej[a], Pavel Kolodziej[a], Leszek Rycerz[a], and Marcelle Gaune-Escard[b]

[a] Chemical Metallurgy Group, Faculty of Chemistry, Wroclaw University of Technology, Wybrzeze Wyspianskiego 27, 50-370 Wroclaw, Poland
[b] Ecole Polytechnique, IUSTI CNRS UMR 6595, Technopole de Chateau-Gombert, 5 rue Enrico Fermi, 13453 Marseille Cedex 13, France

Reprint requests to Prof. M. G.-E.; Fax: +33 4 91 11 74 39;
E-mail: Marcelle.Gaune-Escard@polytech.univ-mrs.fr

Differential scanning calorimetry (DSC) was used to investigate the phase equilibrium in the AgCl-NdCl$_3$ system. This binary mixture represents a typical example of simple eutectic system, with eutectic composition $x(\text{AgCl}) = 0.796$ and temperature $T_{\text{eut}} = 668$ K, respectively. The electrical conductivity of AgCl-NdCl$_3$ liquid mixtures, together with that of pure components was measured down to temperatures below solidification. Results obtained are discussed in terms of possible complex formation.

Key words: Phase Diagram; Electrical Conductivity; Neodymium Chloride; Silver Chloride; Differential Scanning Calorimetry (DSC).

1. Introduction

Phase equilibria in alkali halide-lanthanide halide-based systems, MX-LnX$_3$ (Ln = lanthanide, M = alkali metal, X = halide), are generally complex and characterized by the existence of several stoichiometric compounds. The stability of these compounds depends both on the nature of cations and of the halide X [1 – 3]. Careful analysis of all existing MX-LnX$_3$ phase diagrams has been performed [3] in order to find a relation between the topology of the phase diagrams and the physicochemical properties of the system components. The ionic radii (r_i) and / or charges (e_i) and also their combination, called "ionic potential" $IP = e_i/r_i$, where $e_i = Z_{i\varepsilon}$ (Z_i = valency, ε = elementary charge), were found to be important parameters in this respect [4 – 6]. The ionic potential is a measure of the electric field intensity at the cation surface, therefore accounting for the interaction force of cations with anions. The ratio of the ionic potentials of the alkali metal cation and the lanthanide cation, $IP_{\text{M}^+}/IP_{\text{Ln}^{3+}}$, expresses a comparison of the interaction energies. This ratio influences the phase diagram topology of the MCl-LnCl$_3$, MBr-LnBr$_3$ and MI-LnI$_3$ binary systems. All these systems can be divided into three groups [3]:

– simple eutectic systems ($IP_{\text{M}^+}/IP_{\text{Ln}^{3+}} \geq 0.448$, 0.325 and 0.330 for chloride, bromide and iodide systems, respectively);

– systems including only incongruently melting compounds (in the range $0.280 < IP_{\text{M}^+}/IP_{\text{Ln}^{3+}} < 0.416$, $0.284 < IP_{\text{M}^+}/IP_{\text{Ln}^{3+}} < 0.315$ and $0.306 < IP_{\text{M}^+}/IP_{\text{Ln}^{3+}} < 0.352$ for chloride, bromide and iodide systems, respectively);

– systems including both incongruently and congruently melting compounds ($IP_{\text{M}^+}/IP_{\text{Ln}^{3+}} \leq 0.256$).

This classification was tested on the MBr-CeBr$_3$ binary systems (M = Li, Na, K), which were unknown at this time. Indeed it was found later that LiBr-CeBr$_3$ and NaBr-CeBr$_3$ are simple eutectic systems [7] ($IP_{\text{M}^+}/IP_{\text{Ce}^{3+}} = 0.465$ and 0.366, respectively), whereas in the system KBr-CeBr$_3$ [8] two congruently melting compounds, namely K$_3$CeBr$_6$ and K$_2$CeBr$_5$, exist in agreement with these relations ($IP_{\text{K}^+}/IP_{\text{Ce}^{3+}} = 0.249$) [3].

The rationale to undertake investigations on silver chloride-lanthanide systems was firstly to further test the above topology classification, when a transition metal (silver) chloride is substituted in an alkali metal chloride. Secondly, the high ionic conductivity of some

solid silver halide phases is the reason for their possible application as solid electrolytes [9]. And last, but not least – there is an interest in developing solid state lasers that operate in the middle infrared spectral range [10]. This effort is limited by the availability of host materials that are highly transparent in this range. Silver halide crystals can be attractive candidates for extending laser emission to the mid-IR range. The properties of mixed silver halide crystals such as AgCl$_x$Br$_{1-x}$ have been under active study [11 – 12]. These materials are highly transparent in the near- and mid-IR ranges and have desirable mechanical and optical properties. They may therefore serve as the desirable hosts for mid-IR solid state lasers [10]. Rare earth ions have a complex energy level scheme and some of the optical transitions of these ions are in the mid-IR range. In silver halides, similar transitions or transitions between higher excited states may exist. Incorporating rare earth halides in silver halide crystals and fibers may form a basis for obtaining amplification and lasing in the middle infrared range [10]. Coupling lanthanide and silver halides would possibly offer the same attractive features. So the knowledge of basic, thermodynamic and transport properties of silver halide-lanthanide halide systems would be of significant interest. To the best of our knowledge no data exist on the AgCl-NdCl$_3$ system. Accordingly, we undertook investigations on this binary system. This work reports the phase diagram and electrical conductivity of AgCl-NdCl$_3$ liquid mixtures.

2. Experimental

2.1. Chemicals

Neodymium(III) chloride was synthesized from neodymium(III) oxide (Aldrich 99.9%). Nd$_2$O$_3$ was dissolved in hot concentrated HCl. The solution was evaporated and NdCl$_3 \cdot x$H$_2$O was crystallized. Ammonium chloride was then added (20 mass%) and this wet mixture of hydrated NdCl$_3$ and NH$_4$Cl was first slowly heated to 450 K and then to 570 K to remove the water. The resulting mixture was subsequently heated to 650 K for sublimation of NH$_4$Cl. Finally, the salt was melted at 1100 K under argon atmosphere. Crude NdCl$_3$ was purified by distillation under reduced pressure (~ 0.1 Pa) in a quartz ampoule at 1150 K. NdCl$_3$ prepared in this way was of high purity – min. 99.9%. Chemical analysis was performed by mercurimetric (chlorine) and complexometric (neodymium) meth-

ods. The results were as follows: Nd, $(57.49 \pm 0.13)\%$ $(57.54\%$ calcd.$)$; Cl, $(42.41 \pm 0.12)\%$ $(42.46\%$ calcd.$)$.

Silver chloride was obtained by titration of silver nitrate (POCh Gliwice, p. a.) solution with KCl (Merck Suprapur, min. 99.9%) solution. The prepicitate of AgCl was washed several times with deionized water in order to remove nitrate ions adsorbed on its surface. It was subsequently slowly heated under gaseous HCl atmosphere to 720 K. AgCl prepared in this way was transferred into a glove box and sealed-off in glass ampoules.

The appropriate amounts of NdCl$_3$ and AgCl were melted in vacuum-sealed quartz ampoules. The melts were homogenized and solidified. These samples were ground in an agate mortar in a glove box. Homogeneous mixtures of different compositions were prepared in this way and used in phase diagram and electrical conductivity measurements.

All chemicals were handled under a high purity argon atmosphere in a glove box (water content < 2 ppm). As silver chloride is sensitive to UV-VIS light, all the manipulations were carried out in red light.
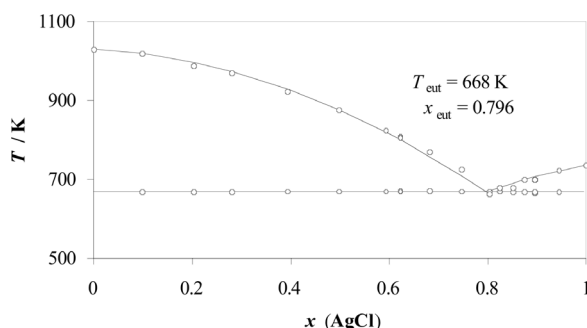
2.2. Measurements

A Setaram DSC 121 differential scanning calorimeter was used to investigate the phase equilibrium in the AgCl-NdCl$_3$ system. The calibration procedure (experimental temperature scale and enthalpy) of the calorimeter was performed as described previously [2, 3]. Samples under investigation (300 – 500 mg) were contained in quartz ampoules (about 6 mm diameter, 15 mm length) sealed under reduced pressure of argon. The sidewalls of ampoules were grounded in order to fit the cells snugly into the heat flow detector. Experiments were conducted at heating and cooling rates ranging from 1 – 5 K min^{-1}.

Electrical conductivity measurements were carried out in capillary quartz cells with cylindrical platinum electrodes, described in details [13]. These cells were calibrated at high temperature with pure molten NaCl [14]. The cell, filled with the substance under investigation, was placed into a stainless steel block to achieve a uniform temperature inside a furnace. The conductivity of the melt was measured by platinum electrodes with the conductivity meter Tacussel CD 810 during increasing and decreasing temperature runs. The mean values of these two runs were used in calculations. Experimental runs were performed at heating and cooling rates of 1 K min^{-1}. The temper-

Table 1. DSC results of the AgCl-NdCl$_3$ binary system.

x(AgCl)	T_{eut} / K Heating	T_{eut} / K Cooling	T_{liq} / K Heating	T_{liq} / K Cooling
0.00	–	–	1029	998
0.0988	667	668	1018	952
0.2034	668	670	988	965
0.2810	668	668	968	943
0.3943	668	670	922	904
0.4976	669	670	876	866
0.5931	668	668	823	811
0.6228	670	671	809	775
0.6818	670	671	769	687
0.7476	669	670	725	689
0.8043	669	663	–	671
0.8240	669	671	678	639
0.8510	668	658	–	680
0.8742	667	652	698	678
0.8957	666	650	699	687
0.9446	667	666	722	716
1	–	–	736	740

Fig. 2. Tammann construction for eutectic determination in the AgCl-NdCl$_3$ system; open circles, experimental results; solid lines, linear fitting of experimental results.
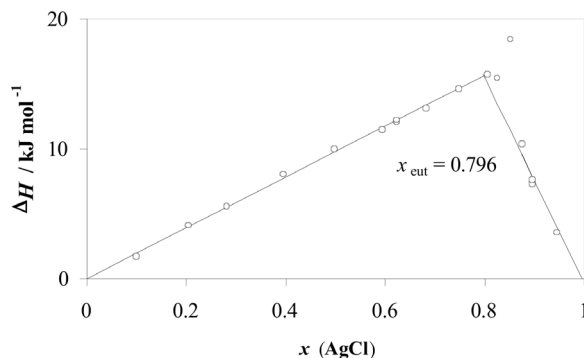

Fig. 1. Phase diagram of the AgCl-NdCl$_3$ system.

ature was measured with a Pt/Pt-Rh(10) thermocouple with 1 K accuracy. Temperature and conductivity data acquisition was made with a PC, interfaced to the conductivity meter. All measurements were carried out under static argon atmosphere. The accuracy of the measurements was about ±2%.

3. Results and Discussion

3.1. Phase Diagram

The AgCl-NdCl$_3$ phase diagram was established for the first time in the present work. DSC investigations were performed on samples with different compositions and yielded both the temperature and the fusion enthalpy of the concerned mixtures. Due to a noticeable supercooling effect during most cooling runs (Table 1), all temperature and enthalpy experimental data reported here were determined from heating curves. The phase diagram presented in Fig. 1 was found to be of the simple eutectic type. In the whole range of

compositions, only two peaks ascribed to the eutectic and the liquidus effects were found in all thermograms. The only exception was in compositions close to the eutectic, where only a single DSC peak was registered. The accuracy in temperature of thermal effects determination was ±1 K. The experimental enthalpy related to the eutectic effect vs. composition plot evidences that no solid solutions formed in the NdCl$_3$-rich part. Thus the corresponding straight line intercepts the composition axis at x(AgCl) = 0. However, the formation of solid solutions cannot be excluded on the AgCl-rich side. Accordingly, the corresponding straight line was not forced to intercept the composition axis at x(AgCl) = 1. The eutectic composition was found to be x(AgCl) = 0.796 ± 0.005 from the intercept of the two linear parts in Fig. 2 (Tammann plot), described by the equations

$$\Delta_{fus}H_m = 19.632x \text{ and}$$
$$\Delta_{fus}H_m = 78.719 - 79.096x \text{ (in kJ mol}^{-1}\text{),} \quad (1)$$

where x denotes the AgCl molar fraction. The eutectic temperature determined from all appropriate DSC curves was found to be 668 K, whereas the enthalpy of fusion at the eutectic composition was (15.7 ± 0.7) kJ mol^{-1}. The AgCl molar fractions at which solid solutions may exist at 668 K was found also from the Tammann diagram (Fig. 2) as $x \geq 0.995$.

3.2. Electrical Conductivity

The variation of molten salt resistance R_{exp} with frequency f can be expressed by

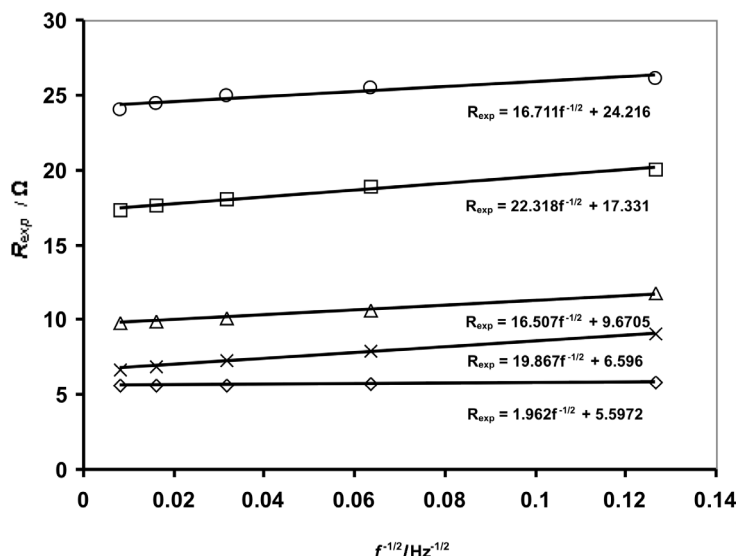$$R_{exp} = R_{inf} + \frac{C}{\sqrt{f}}, \quad (2)$$

Fig. 3. Resistance variation with frequency for a few mixtures under investigation; open circles and diamonds, NdCl$_3$ and AgCl, respectively; squares, triangles and crosses, AgCl-NdCl$_3$ liquid mixtures with molar fractions of NdCl$_3$ of 0.800, 0.600, and 0.308, respectively.
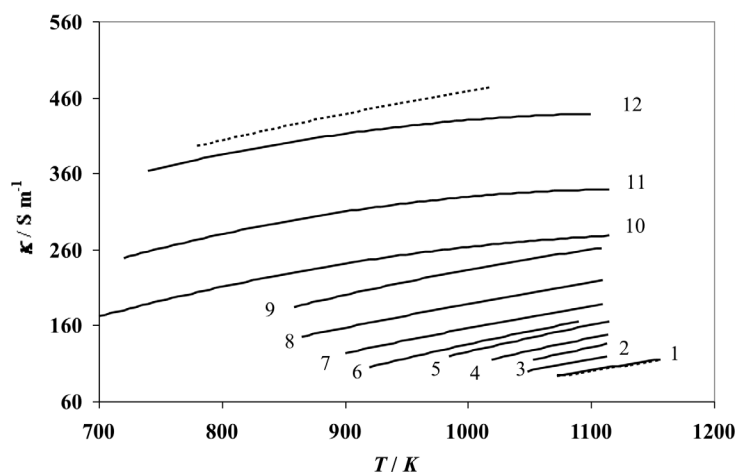

Fig. 4. Electrical conductivity of molten AgCl-NdCl$_3$ mixtures vs. temperature; 1, NdCl$_3$ (dashed line – literature data [16]); 12, AgCl (dashed line – literature data [14]); 2 to 11, liquid AgCl-NdCl$_3$ mixtures with NdCl$_3$ molar fractions of 0.952, 0.894, 0.800, 0.700, 0.600, 0.500, 0.400, 0.308, 0.202, and 0.091, respectively.

where R_{inf} polarization-free resistance at infinite frequency and C is a constant characteristic of the melt under investigation. It contains polarization resistance and electrolyte capacitance terms, which were found to be proportional to $f^{-1/2}$ [15]. Thus (2) was used in processing all resistance data obtained in this work. Electrical conductivity measurements were carried out at the frequency 4 kHz and R_{inf} was calculated from (2). The value of C, necessary in this calculation, was determined from the frequency dependence of resistance, which was obtained from measurements carried out on the frequency range from 60 Hz to 16 kHz. Figure 3 shows the resistance variation with frequency for NdCl$_3$, AgCl and some AgCl-NdCl$_3$ liquid mixtures.
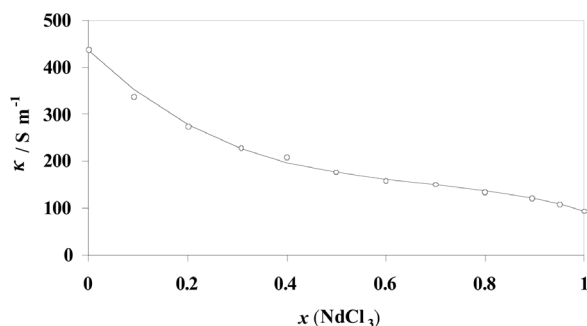
The electrical conductivity of AgCl-NdCl$_3$ liquid mixtures was measured for the first time over the entire composition range in steps of about 10 mol%. Prior to these measurements, the conductivity of pure components was determined. Our conductivity data on NdCl$_3$ agree quite well with data of Potapov et al. [16] with a deviation not exceeding 1.5% over the entire temperature range (Fig. 4). Our results on AgCl are lower than those reported by Doucet and Bizouard [14]. This difference increases with temperature from 4.5% at 785 K up to about 6% at 1020 K.

A second-order polynomial dependence of conductivity κ on temperature was applied to all experimental results:

$$\kappa = A + B \cdot T + C \cdot T^2 \text{ (in S m}^{-1}). \tag{3}$$

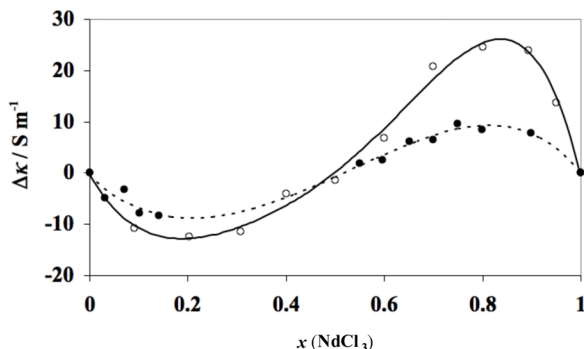Table 2. Coefficients in equation: $\kappa = A + B \cdot T + C \cdot T^2$ for AgCl-NdCl$_3$ liquid mixtures.

x(NdCl$_3$)	$A \cdot 10^{-3}$ / S m^{-1}	B / S m^{-1} K^{-1}	$C \cdot 10^3$ / S m^{-1} K^{-2}	Temp. range / K
1.000	−0.2321	0.3519	−0.0446	1158 − 1072
0.951	−1.7540	3.1571	−1.3251	1117 − 1048
0.894	−0.1011	0.0702	0.1281	1115 − 1053
0.800	−0.8152	1.4321	−0.5102	1116 − 1019
0.700	−0.3931	0.6660	−0.1480	1115 − 985
0.600	−0.4840	0.8851	−0.2661	1094 − 920
0.500	−0.3581	0.7203	−0.2063	1113 − 900
0.400	−0.2552	0.5881	−0.1450	1112 − 865
0.308	−0.4150	0.9480	−0.3241	1109 − 859
0.202	−0.3421	1.0332	−0.4280	1119 − 700
0.091	−0.3230	1.1601	−0.5083	1115 − 720
0.000	−0.1761	1.0800	−0.4742	1100 − 775

Fig. 5. Electrical conductivity isotherm of AgCl-NdCl$_3$ liquid mixtures at 1070 K.

The electrical conductivity dependence on temperature is shown in Fig. 4 for AgCl, NdCl$_3$ and ten AgCl-NdCl$_3$ mixtures. The coefficients A, B, and C of (3) are displayed in Table 2. In Fig. 5 the conductivity isotherm at 1070 K is plotted against the mole fraction of NdCl$_3$. The specific conductivity decreases with increase of the NdCl$_3$ concentration, with significantly larger changes in the AgCl-rich region, as it is expected. A decrease of the AgCl molar fraction causes a decrease of the number of mobile ions (Ag$^+$, Cl$^-$), which are carriers of electrical charge.

It is obvious that a simple additivity law is not applicable to the electrical conductivity of molten salt mixtures even in the case of the simplest melts (without chemical interaction) [17]. The commonly observed deviation from additivity can result from physical and chemical interactions between components of the melt. In many cases the composition dependence of the specific conductivity can be well represented by the Kuroda [18] equation for binary mixtures

$$\kappa = x_1{}^2\kappa_1 + x_2{}^2\kappa_2 + 2x_1 x_2 \kappa_1, \tag{4}$$

Fig. 6. Relative deviations of the electrical conductivity from the Kuroda equation (5) for AgCl-NdCl$_3$ and NaCl-NdCl$_3$ liquid mixtures; open circles and solid line, AgCl-NdCl$_3$; black circles and dashed line, NaCl-NdCl$_3$.

where x_1, x_2 are the mole fractions of the pure components, and κ_1, κ_2 are their specific conductivities, with $\kappa_1 < \kappa_2$. However, in the case of the liquid mixtures investigated here, significant deviations of experimental results from this equation were observed. These relative deviations, calculated according to

$$\Delta\kappa = \frac{\kappa_{exp} - \kappa_{Kuroda}}{\kappa_{Kuroda}} \cdot 100\%, \tag{5}$$

are presented in Figure 6.

Negative deviations occur in the AgCl-rich composition range (minimum at $\sim 20-25$ mol% NdCl$_3$), and are followed by positive deviations starting from about 50 mol% NdCl$_3$ (maximum at ~ 85 mol%). We have applied (4) to the literature conductivity data of NaCl-NdCl$_3$ liquid mixtures [16] because of the similarity of Ag$^+$ and Na$^+$ ionic radii (100 and 102 pm, respectively). The results of this calculation are also presented in Figure 6. The behaviour of NaCl-NdCl$_3$ liquid mixtures is almost identical to that of AgCl-NdCl$_3$, both in the sense of negative and positive deviations and of their minimum and maximum location.

According to [17, 19], marked negative electrical conductivity deviations are strongly indicative of complex formation. If only one complex species exists in the melt, the absolute value of deviation reaches a maximum at the composition corresponding to the stoichiometry of this complex. If several complex species co-exist, the location of the minimum may slightly deviate from the exact stoichiometry of the predominant species. Therefore the existence of negative deviations in AgCl-NdCl$_3$ liquid mixtures with a minimum x(NdCl$_3$) ≈ 0.25 is indicative of [NdCl$_6$]$^{3-}$ octahedral complexe formation in the melt. Unfortunately no ex-

perimental confirmation of its existence exists so far. However, taking into account the similarity of Ag^+ and Na^+ ionic radii, the results of different experimental techniques applied to the NaCl-NdCl₃ liquid system may bring further arguments about this hypothetical $[NdCl_6]^{3-}$ complexe formation in the system with silver chloride. Raman spectroscopic investigations [20] showed that octahedral $[LnCl_6]^{3-}$ ions are formed in MCl-LnCl₃ liquid mixtures (M = alkali metal). These ions constitute the predominant species in MCl-rich liquid mixtures. As the LnCl₃ concentration increases, distortion of octahedra, which are bridged by chloride anions, takes place. Neodymium(III) complex formation in molten NaCl, KCl, RbCl, CsCl and (Li-K)Cl$_{eut}$ was evidenced by electronic spectroscopy [21]. Predominant octahedral local symmetry of Nd^{3+} was found over the entire composition range including pure molten NdCl₃. The formation of these $[LnCl_6]^{3-}$ complexes influences the electrical conductivity and induces the appearance of the negative deviation in the system NaCl-NdCl₃. The mixing enthalpy measurements performed on MCl-NdCl₃ liquid mixtures [22] also suggested the existence of these octahedral complexes. Therefore, it is not unreasonable to assume that $[NdCl_6]^{3-}$ complexes also exist in the AgCl-NdCl₃ liquid mixture. Accordingly, the minimum of negative electrical conductivity deviations from (4) is located at a NdCl₃ molar fraction of about 0.25. The positive deviations at NdCl₃-rich compositions are apparently caused by the disruption of associates in pure NdCl₃, resulting in a new structure in which neodymium chloride contributes more to the transfer of electricity.

The different magnitude of both negative and positive deviations in NaCl-NdCl₃ and AgCl-NdCl₃ mixtures is apparently caused by the different nature of Na^+ and Ag^+ ions. The role of sodium chloride or silver chloride is to provide additional chloride ions to enable Nd^{3+} to expand its coordination shell. But there is competition between M^+ and Nd^{3+} for Cl^- in the ionic environment. Na^+ (hard Lewis acid) with a noble gas configuration, has a spherical symmetry and low polarizable hard sphere. Its electronic cloud is rigid and prefers ionic bonding. On the other hand, Ag^+ with d^{10} electron structure (soft Lewis acid) has a highly polarizable soft sphere. High quadrupolar polarizability (deformation from sphere into an ellipsoid) takes place in this ion [23]. Accordingly Na^+ is more chloride attracting than Ag^+, or in other words, AgCl is a better "donor" of chloride ions than NaCl. Thus in AgCl-rich melts the amount of $[NdCl_6]^{3-}$ complexes formed is larger than in NaCl-rich mixtures, hence the larger negative deviations of electrical conductivity in the AgCl-NdCl₃ system. In NdCl₃-rich mixtures a disruption of the polymeric structure takes place. It will be more marked in the case of good chloride ion donors (AgCl) and results in a larger positive electrical conductivity deviation than in the NaCl-NdCl₃ melt.

[1] H. J. Seifert, J. Therm. Anal. Cal. **7**, 789 (2002).
[2] L. Rycerz, High Temperature Characterization of LnX₃ and LnX₃-AX Solid and Liquid Systems (Ln = Lanthanide, A = Alkali, X = Halide): Thermodynamics and Electrical Conductivity, Ph. D. Thesis, Marseille 2003.
[3] L. Rycerz, Sci. Pap. Inst. Inorg. Chem. Metallurgy of Rare Elements, Wroclaw Univ. Technol., Ser. Monogr. **35** (2004) (in Polish).
[4] W. Gawel, Roczniki Chem. **49**, 699 (1975).
[5] W. Gawel and J. Josiak, Bull. Pol. Ac.: Chem. **42**, 211 (1994).
[6] W. Gawel, J. Nucl. Mater. **247**, 301 (1997).
[7] E. Ingier-Stocka, L. Rycerz, S. Gadzuric, and M. Gaune-Escard, J. Alloys Comp. **450**, 162 (2008).
[8] L. Rycerz, E. Ingier-Stocka, S. Gadzuric, and M. Gaune-Escard, Z. Naturforsch. **62a**, 197 (2007).

[9] C. S. Sunandana and P. Senthil Kumar, Bull. Matter. Sci. **27**, 1 (2004).
[10] L. Nagli, A. German, and A. Katzir, Opt. Mater. **13**, 89 (1999).
[11] D. Bunimowich, L. Nagli, and A. Katzir, Opt. Lett. **20**, 2417 (1995).
[12] L. Nagli, D. Bunimovich, A. Schmilevich, N. Kristianpoller, and A. Katzir, J. Appl. Phys. **74**, 5737 (1993).
[13] Y. Fouque, M. Gaune-Escard, W. Szczepaniak, and A. Bogacz, J. Chim. Phys. **75**, 360 (1978).
[14] Y. Doucet and M. Bizouard, Compt. Rend. **250**, 73 (1960).
[15] R. P. T. Tomkins, G. J. Janz, and E. Andalaft, J. Electrochem. Soc. Electrochem. Sci. Technol. **117**, 906 (1970).

[16] A. Potapov, L. Rycerz, and M. Gaune-Escard, Z. Natur-forsch. **62a**, 431 (2007).

[17] Yu. K. Delimarskii and B. F. Markov, Electrochemistry of Fused Salts, The Sigma Press Publishers, Washington 1961.

[18] J. Mochinaga, K. Cho, and T. Kuroda, Denki Kagaku **36**, 746 (1968).

[19] Yu. K. Delimarskii, Elektrokhimiia ionnyh rasplavov, Mietallurgiia, Moskva 1978 (in Russian).

[20] G. M. Photiadis, B. Borresen, and G. N. Papatheo-dorou, J. Chem. Soc. Faraday Trans. **17**, 2605 (1998).

[21] Yu. A. Barbanel, Coordination Chemistry of f-Elements in Melts, Energoatomizdat, Moscow 1985 (in Russian).

[22] M. Gaune-Escard, L. Rycerz, A. Bogacz, and W. Szczepaniak, Thermochim. Acta **236**, 67 (1994).

[23] L. M. Slifkin, Cryst. Lattice Defects Amorphous Mater. **18**, 81 (1989).